Euro. Jnl of Applied Mathematics (2001), *vol.* 12, *pp.* 677–688. Printed in the United Kingdom

Hele-Shaw flows with free boundaries in a corner or around a wedge Part II: Air at the vertex

S. RICHARDSON

Department of Mathematics and Statistics, University of Edinburgh, James Clerk Maxwell Building, Mayfield Road, Edinburgh EH9 3JZ, Scotland

(*Received 18 September 2000; revised 15 March 2001*)

Consider a Hele-Shaw cell with the fluid (liquid) confined to an angular region by a solid boundary in the form of two half-lines meeting at an angle $\alpha\pi$; if $0 < \alpha < 1$ we have flow in a corner, while if $1 < \alpha \leqslant 2$ we have flow around a wedge. We suppose contact between the fluid and each of the lines forming the solid boundary to be along a single segment that does not adjoin the vertex, so we have air at the vertex, and contemplate such a situation that has been produced by injection at a number of points into an initially empty cell. We show that, if we assume the pressure to be constant along the free boundaries, the region occupied by the fluid is the image of a rectangle under a conformal map that can be expressed in terms of elliptic functions if $\alpha = 1$ or $\alpha = 2$, and in terms of theta functions if $0 < \alpha < 1$ or $1 < \alpha < 2$. The form of the function giving the map can be written down, and the parameters appearing in it then determined as the solution to a set of transcendental equations. The procedure is illustrated by a number of examples.

1 Introduction

In a recent paper (Richardson, 2001b), a class of flows with time-dependent free boundaries in a Hele-Shaw cell was considered, the motion being confined to an angular region by solid boundaries in the form of two half-lines meeting at an angle $\alpha\pi$; we have flow in a corner if $0 < \alpha < 1$, and flow around a wedge if $1 < \alpha \leqslant 2$. A condition of constant pressure was supposed to be applicable at the free boundary, and the scenario examined was such that it could be produced by injection at a number of points into an initially empty cell. An essential assumption was that the fluid be in contact with each of the lines forming the solid boundary along a single segment emanating from the vertex. In particular, if we think of the injected fluid as a liquid, there must be no air trapped near the vertex. In the present paper, we consider the situation when air *is* trapped near the vertex. The region occupied by the fluid (liquid) is now in contact with each of the lines forming the solid boundary along a single segment that does not adjoin the vertex, and there are two free boundaries.

2 Basic formulation

The configuration we are considering is illustrated in the z-plane of Figure 1, where $z = x + iy$. The fluid region D is bounded by the portion DA of the half-line $\arg z = 0$,

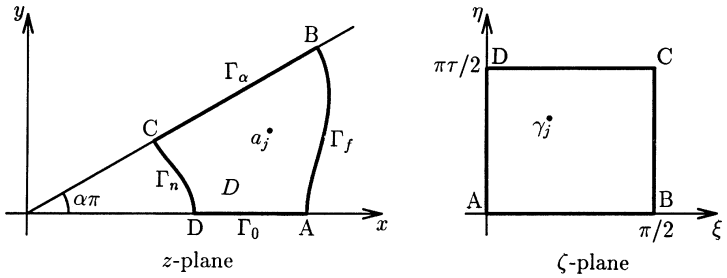

FIGURE 1. The z-plane and ζ-plane used in the analysis.

denoted by Γ_0, the portion BC of the half-line $\arg z = \alpha\pi$, denoted by Γ_α, the free boundary CD that is nearest the vertex, denoted by Γ_n, and the free boundary AB that is furthest from the vertex, denoted by Γ_f. We suppose this state to have been reached by injecting an area πr_j^2 at the injection point $z = a_j$ for $j = 1, 2, \ldots, N$, the cell being initially empty.

If $\alpha = 1/n$ for some positive integer n, we can invoke images and consider an equivalent problem involving a doubly-connected blob of fluid in the z-plane, with no solid boundaries present. A situation of this kind, with $\alpha = 1/2$, was considered by Richardson (1994). If α is not of this special form, we can still invoke images to satisfy the relevant boundary condition on the solid boundaries, but this now extends the flow onto a Riemann surface. The global structure of this surface depends on the nature of α, so we attempt to express the arguments in a local form that is applicable to all values of α. We may contemplate the Cauchy transform for the fluid region extended over the Riemann surface, but use only a knowledge of its singularities, as was done in Richardson (2001b).

Let $z = f(\zeta)$ map the rectangle with corners at $\zeta = 0, \pi/2, \pi/2 + \pi\tau/2$ and $\pi\tau/2$ conformally onto D. We have $\zeta = \xi + i\eta$, and the ζ-plane is illustrated in Figure 1 where points labelled with the same letter in the z-plane and ζ-plane correspond under the map. For any such D, there is a map with these properties for some determinate value of τ. Here τ is purely imaginary and has a positive imaginary part, this notation being adopted to accord with the standard usage in the literature of the theta functions to which the analysis will lead. Rainville (1971) gives a convenient account of the basic properties of these functions. We also employ the usual additional variable q related to τ by

$$q = e^{\pi i \tau}, \tag{2.1}$$

so here q is real and $0 < q < 1$. It will transpire that the particular cases $\alpha = 1$ and $\alpha = 2$ are exceptional, and require a separate treatment for which a different choice of scaling in the ζ-plane is more convenient. However, we will couch the general discussion in terms that are appropriate for the situation sketched in Figure 1, and make adjustments later when necessary.

Suppose the points $\zeta = \gamma_j$ map to the injection points $z = a_j$, so

$$f(\gamma_j) = a_j \quad \text{for } j = 1, 2, \ldots, N. \tag{2.2}$$

The line DA in the z-plane, on which $z = \bar{z}$, corresponds to the line DA in the ζ-plane,

https://doi.org/10.1017/S0956792501004570 Published online by Cambridge University Press

on which $\zeta = -\overline{\zeta}$, so there

$$f(\zeta) = \overline{f(-\overline{\zeta})}, \tag{2.3}$$

a relationship that allows $f(\zeta)$ to be analytically continued across DA in the ζ-plane.

The line BC in the z-plane, on which $z = e^{2i\alpha\pi}\,\overline{z}$, corresponds to BC in the ζ-plane, on which $\zeta = -\overline{\zeta} + \pi$, so there

$$f(\zeta) = e^{2i\alpha\pi}\,\overline{f(-\overline{\zeta} + \pi)}, \tag{2.4}$$

a relationship that allows $f(\zeta)$ to be analytically continued across BC in the ζ-plane.

If, now, we replace ζ by $\zeta + \pi$ in (2.4) and compare the result with (2.3), we see that we have

$$f(\zeta + \pi) = e^{2i\alpha\pi} f(\zeta), \tag{2.5}$$

a relationship that now allows $f(\zeta)$ to be analytically continued into the entire strip $0 < \eta < \pi|\tau|/2$.

Consider the Cauchy transform of the region D plus its images on a Riemann surface – if such a surface that is not just part of the z-plane be necessary. As in Richardson (2001b), we obtain a function $h_e(z)$ with simple poles at the injection points where

$$h_e(z) = \frac{r_j^2}{z - a_j} + O(1) \quad \text{as } z \to a_j. \tag{2.6}$$

The analogue of (1.5) in Richardson (2001b) now allows us to analytically continue $f(\zeta)$ across both AB, on which $\zeta = \overline{\zeta}$, and CD, on which $\zeta = \overline{\zeta} + \pi\tau$, in the ζ-plane, and this tells us that

$$f(\zeta + \pi\tau) = f(\zeta), \tag{2.7}$$

which now allows $f(\zeta)$ to be analytically continued into the entire ζ-plane. We also find that $f(\zeta)$ has a simple pole at $\zeta = \overline{\gamma}_j$ – or, equivalently, that $\overline{f(\overline{\zeta})}$ has a simple pole at $\zeta = \gamma_j$. Moreover, if

$$\overline{f(\overline{\zeta})} = \frac{\beta_j}{\zeta - \gamma_j} + O(1) \quad \text{as } \zeta \to \gamma_j, \tag{2.8}$$

equivalent to

$$f(\zeta) = \frac{\overline{\beta}_j}{\zeta - \overline{\gamma}_j} + O(1) \quad \text{as } \zeta \to \overline{\gamma}_j, \tag{2.9}$$

a comparison of residues implies that

$$\beta_j f'(\gamma_j) = r_j^2 \quad \text{for } j = 1, 2, \ldots, N. \tag{2.10}$$

The arguments used here are exactly the same as those used in Richardson (1994) and § 2 of Richardson (2000). Note that, from (2.3) and (2.8), we can deduce that

$$f(\zeta) = -\frac{\beta_j}{\zeta + \gamma_j} + O(1) \quad \text{as } \zeta \to -\gamma_j. \tag{2.11}$$

If $\alpha = 1$ or $\alpha = 2$ we have $e^{2i\alpha\pi} = 1$, so (2.5) and (2.7) then imply that $f(\zeta)$ has both π and $\pi\tau$ as periods, and is therefore an elliptic function. We set aside these two special

https://doi.org/10.1017/S0956792501004570 Published online by Cambridge University Press

values of α for the moment, and thus have $e^{2i\alpha\pi} \neq 1$. Then $f(\zeta)$ has $\pi\tau$ as a period, but acquires a multiplicative factor that is not 1 when its argument is increased by π. The map can then be expressed in terms of the standard theta function $\theta_1(\zeta, q) = \theta_1(\zeta)$ defined by

$$\theta_1(\zeta) = 2\sum_{n=0}^{\infty}(-1)^n q^{\left(n+\frac{1}{2}\right)^2}\sin(2n+1)\zeta. \tag{2.12}$$

Recall that in our application we have $0 < q < 1$, and the series here then converges for all values of ζ. We have

$$\theta_1(\zeta + \pi) = -\theta_1(\zeta), \tag{2.13}$$

and

$$\theta_1(\zeta + \pi\tau) = -q^{-1}e^{-2i\zeta}\theta_1(\zeta). \tag{2.14}$$

One can show (see Rainville (1971) for example) that $\theta_1(\zeta)$ has zeros at, and only at, the points $\zeta = m\pi + n\pi\tau$ for m and n integers, and these are all simple zeros.

The functions we seek are *doubly-periodic functions of the second kind* in the terminology introduced by Hermite, and he gave an effective method for their construction; see Hermite (1912). Following these ideas, we consider the function

$$g(\zeta) = \frac{\theta_1'(0)\,\theta_1(\zeta + \alpha\pi\tau)}{\theta_1(\alpha\pi\tau)\,\theta_1(\zeta)}\,e^{2i\alpha\zeta}. \tag{2.15}$$

Recall that we are supposing α to be neither 1 nor 2, so the factor $\theta_1(\alpha\pi\tau)$ in the denominator here does not vanish, and the zeros of $\theta_1(\zeta)$ in the denominator do not cancel with zeros of $\theta_1(\zeta + \alpha\pi\tau)$ in the numerator. Thus $g(\zeta)$ has simple poles at the points $\zeta = m\pi + n\pi\tau$ for m and n integers, and these are its only singularities. The factors $\theta_1'(0)$ and $\theta_1(\alpha\pi\tau)$ are inserted to ensure that we have a residue of 1 at the simple pole at $\zeta = 0$. Using (2.13) and (2.14), one easily checks that $g(\zeta)$ satisfies the same equations (2.5) and (2.7) that $f(\zeta)$ must satisfy.

The sole singularities of $f(\zeta)$ in the rectangle $-\pi/2 < \xi < +\pi/2, -\pi|\tau|/2 < \eta < +\pi|\tau|/2$ are to be simple poles at the points $\zeta = \overline{\gamma}_j$ with residue $\overline{\beta}_j$, as dictated by (2.9), and simple poles at the points $\zeta = -\gamma_j$ with residue $-\beta_j$, as dictated by (2.11). It therefore follows that

$$f(\zeta) = \sum_{j=1}^{N}\left\{\overline{\beta}_j g(\zeta - \overline{\gamma}_j) - \beta_j g(\zeta + \gamma_j)\right\}. \tag{2.16}$$

Consider now the exceptional cases $\alpha = 1$ and $\alpha = 2$. The function $f(\zeta)$ is then elliptic, with both π and $\pi\tau$ as periods, according to (2.5) and (2.7). However, to express the results in their simplest form using the standard notations of the theory of Jacobian elliptic functions, we use a different scaling in the ζ-plane of Figure 1 that places B at $\zeta = K$ and D at $\zeta = iK'$, where $K = K(k)$ is the complete elliptic integral of the first kind with modulus k, and $K' = K'(k) = K(k')$ with $k' = \sqrt{1-k^2}$ is its complement. Here $0 < k < 1$ and $0 < k' < 1$. Bowman (1961) is a useful reference for the properties of elliptic functions.

With this modified ζ-plane, $f(\zeta)$ now has $2K$ and $2iK'$ as periods and, since we have only simple poles, it can be expressed as a sum involving only Jacobi's zeta function $Z(\zeta, k) = Z(\zeta)$. This has a simple pole of residue 1 at $\zeta = iK'$, so $Z(\zeta - iK')$ plays the

rôle of $g(\zeta)$ in (2.16). However, $Z(\zeta)$ itself is *not* an elliptic function (it cannot be, for it has only one pole in any fundamental parallelogram), and has $2K$ as a period, but $2iK'$ as a quasi-period—that is, it acquires an additive increment when $2iK'$ is added to its argument. Linked to this is the fact that the residues at the poles of an elliptic function cannot be arbitrarily assigned; the sum of the residues at the poles in any fundamental parallelogram must be zero. In the present situation, this means that

$$\sum_{j=1}^{N} \operatorname{Im} \beta_j = 0. \tag{2.17}$$

Note that there is *no* such restriction on the β_j in the circumstances to which (2.16) applies. Now we have

$$f(\zeta) = \sum_{j=1}^{N} \left\{ \overline{\beta}_j Z(\zeta - iK' - \overline{\gamma}_j) - \beta_j Z(\zeta - iK' + \gamma_j) \right\} + \delta, \tag{2.18}$$

where δ is a real constant; that δ must be real is a consequence of the fact that $Z(\zeta)$ is an odd function that is real for real ζ, and the requirement that $f(\zeta)$ must satisfy (2.3). This expression for $f(\zeta)$ has $2K$ as a period because $Z(\zeta)$ has this as a period too, and has $2iK'$ as a period in spite of the fact that $Z(\zeta)$ has this only as a quasi-period by virtue of (2.17). Note the presence of the additive constant δ in (2.18) that is not present in (2.16). This difference arises because any constant function is elliptic, but the only constant function that satisfies both (2.5) and (2.7) when $e^{2i\alpha\pi} \neq 1$ is the zero function. Thus, when $\alpha = 1$ or $\alpha = 2$ there is one extra parameter δ in the formula for $f(\zeta)$, but there is also the extra condition (2.17) on those parameters to compensate. That there should be this extra parameter in these circumstances is not too surprising if one just thinks in terms of the geometry; when $\alpha = 1$ or $\alpha = 2$, we still have a situation of the kind we are considering if we translate the z-plane of Figure 1 in the x-direction, but this is not so for other values of α where the origin has a special significance.

In fact, as is to be expected, we still require one further equation. Those we have exploited thus far take into account the assumption that there is a constant pressure along each of the two free boundaries, but still allow those two pressures to be different. We need an equation that takes into account the physics of the air near the vertex. If we suppose this air to be incompressible and unable to escape, we simply require that the area between $\arg z = 0, \arg z = \alpha\pi$, and the free boundary CD in the z-plane of Figure 1, remain constant; one can compute the pressure difference between the free boundaries CD and AB that is necessary to bring about this state of affairs if desired, but it is not required to solve for the motion. There is a difficulty with this incompressibility assumption that is examined in some detail by Richardson (1994): as a specific example of this, if we inject into an initially empty corner with $0 < \alpha < 1/2$, there is no solution beyond the instant when the air first becomes trapped within the constraints of our model. But in the injection moulding context, when attempting to fill a mould with liquid, there is an air vent at the vertex, and the pressures on the two free boundaries are thereby kept equal. It is this assumption on which we will concentrate here, though it should be clear that we could proceed with alternatives.

This complication with two free boundaries also arises when we have a doubly-

connected fluid region and no solid boundaries (Richardson, 1994) or a fluid region confined to an infinite strip (Richardson, 1996), and the computations required here are similar to those in these two references. (The configuration in the latter reference may be thought of as the limit $\alpha \to 0$ of that discussed here, though some care is needed to effect this limit in our formulae.) The basic flow we are considering in the z-plane of Figure 1 is governed by a function $\phi(x, y)$ that is harmonic in D except for logarithmic singularities at the injection points $z = a_j$. This function is a multiple of the pressure, and its gradient gives us the velocity field. Thus we have $\partial\phi/\partial n = 0$ on Γ_0 and Γ_α. If we allow, for the moment, the pressure to have *different* constant values on the two free boundaries, we have $\phi = \phi_n$ on Γ_n and $\phi = \phi_f$ on Γ_f for some constants ϕ_n and ϕ_f. Now let $l(x, y)$ be any function that is harmonic on the closure of D and does not depend on time, t, and define

$$L(t) = \iint_{D(t)} l(x, y)dx\,dy, \tag{2.19}$$

where we have now emphasized the dependence of D on t in our notation. Using Green's theorem, we find that

$$\frac{dL}{dt} = \phi_n \int_{\Gamma_n} \frac{\partial l}{\partial n}\,ds + \phi_f \int_{\Gamma_f} \frac{\partial l}{\partial n}\,ds + \int_{\Gamma_0 \cup \Gamma_\alpha} \phi\,\frac{\partial l}{\partial n}\,ds + \sum_{j=1}^{N} Q_j\, l(a_j), \tag{2.20}$$

with an evident interpretation of $l(a_j)$, where Q_j is the rate at which area is being injected at $z = a_j$.

When we have *no* pressure difference, we can take $\phi_n = \phi_f = 0$, and the first two terms on the right-hand side of (2.20) disappear. The result we require arises by taking $l(x, y) = \log|z|$ in this equation; the third term on the right-hand side then vanishes too. The result can then be integrated with respect to time, for Q_j is just the rate of change of πr_j^2. Assuming that we begin the injection with an empty cell, we obtain

$$\iint_D \log|z|dx\,dy = \pi \sum_{j=1}^{N} r_j^2 \log|a_j|. \tag{2.21}$$

The fact that in the initial stages of this motion the D in question is not connected if $N > 1$ (to begin with, it is a collection of circular discs about the injection points), and is not in contact with the solid boundaries, does not interfere with the logic of this argument.

For use in the computations, equation (2.21) must be expressed in terms of the mapping function $f(\zeta)$. The integral on the left-hand side of (2.21) is the real part of the integral of $\log z$ over D, and this can be written as an integral round the boundary of D using Green's theorem. The contribution from some parts of this boundary can be explicitly evaluated, and the other contributions are evaluated as integrals in the ζ-plane. The result can be written, with an evident notation, as

$$\frac{1}{2}\,\mathrm{Im} \int \overline{f(\zeta)} \log\{f(\zeta)\} f'(\zeta)\,d\zeta - \frac{1}{4}\alpha\pi\left\{|f(\mathrm{B})|^2 - |f(\mathrm{C})|^2\right\} = \pi \sum_{j=1}^{N} r_j^2 \log|a_j|, \tag{2.22}$$

where the integral is along the two line segments from A to B and from C to D (note the directions) in the ζ-plane of Figure 1.

https://doi.org/10.1017/S0956792501004570 Published online by Cambridge University Press

If α is neither 1 nor 2, there are $2N$ complex parameters β_j and γ_j in our formula (2.16) giving the conformal map, plus the purely imaginary parameter τ or the real parameter q related to τ by (2.1), whichever one chooses to work with. To find these, we have the $2N$ complex equations (2.2) and (2.10), plus the real equation (2.22). If α is equal to 1 or 2, formula (2.16) is replaced by (2.18) with one extra real parameter δ, but we have the extra real equation (2.17). In all cases, we have just sufficient equations to determine the parameters, and the examples in §3 will show that we have a viable solution routine.

When we inject into a corner of angle $\alpha\pi < \pi/2$ and trap air in the corner, we expect this air to be expelled if there is an air vent at the vertex, and we reach a situation that can be analysed by the methods of Richardson (2001b). To determine exactly *when* all the air is expelled, we need to add to the equations in this reference the relevant form of (2.22). We find this to be

$$\frac{1}{2}\,\mathrm{Im}\int \overline{f(\zeta)}\log\{f(\zeta)\}f'(\zeta)\,d\zeta - \frac{1}{4}\alpha\pi|f(-1)|^2 = \pi\sum_{j=1}^{N} r_j^2\log|a_j|, \tag{2.23}$$

where $f(\zeta)$ is now the mapping function appearing in Richardson (2001b), and the integral is taken round the semicircle AB in the ζ-plane of Figure 1 therein.

We have already remarked that, when $\alpha = 1/n$ for some positive integer n, the problem can be solved by images in the original z-plane, and one can show that the solution obtained by this means is equivalent to that found using the present approach. One may also consider the limiting form of the present solution as the air trapped near the vertex disappears, and show that it then agrees with the solution in Richardson (2001b). This limit involves $\tau \to i\infty$ in the ζ-plane of Figure 1, or $K' \to \infty$ so $k \to 0$ if $\alpha = 1$ or $\alpha = 2$. Since $K \to \pi/2$ as $k \to 0$, in all cases the ζ-plane used here degenerates to a semi-infinite strip of width $\pi/2$, and this must be mapped to the semidisc used in the ζ-plane of Richardson (2001b). In fact, there is a subtlety involved in this limit that is, perhaps, best seen by considering formula (2.18); this is supposed to describe the situation for both $\alpha = 1$ and $\alpha = 2$, but the limit must be quite different in the two cases! With $f(\zeta)$ now used to denote the function giving the limiting form of the map needed with a semidisc in the ζ-plane, we require $f(\zeta) = O(\zeta^2)$ for $\alpha = 2$ but $f(\zeta) = O(\zeta)$ for $\alpha = 1$, as $\zeta \to 0$. In fact, a formal limiting process leads to a local expansion for $f(\zeta)$ of the form $f(\zeta) = \zeta(a + b\,\zeta + c\,\zeta^2 + \cdots)$, and we find that $a \neq 0$ if $\alpha = 1$, but $a = 0$ if $\alpha = 2$. There is a similar puzzle, with a similar solution, when α has other values, for as $\tau \to i\infty$ we have

$$g(\zeta) \to \begin{cases} \dfrac{e^{-i\zeta}}{\sin\zeta}\,e^{2i\alpha\zeta} & \text{if} \quad 0 < \alpha < 1\,, \\[2ex] \dfrac{e^{-i\zeta}}{\sin\zeta}\,e^{2i(\alpha-1)\zeta} & \text{if} \quad 1 < \alpha < 2\,. \end{cases} \tag{2.24}$$

These results are most easily obtained from (2.15) by first expressing the theta functions as infinite products; see Rainville (1971). Thus the limiting form for $g(\zeta)$ if $1 < \alpha < 2$ is actually the same as that for $g(\zeta)$ with α replaced by $\alpha - 1$. (This is not too surprising geometrically, for $\arg z = \alpha\pi$ and $\arg z = (\alpha - 1)\pi$ just describe two halves of the same line.) Now we need the function $f(\zeta)$ when we are concerned with the map from the semidisc to be such that $f(\zeta) = O(\zeta^\alpha)$ as $\zeta \to 0$ for *all* α. Using a formal limiting

https://doi.org/10.1017/S0956792501004570 Published online by Cambridge University Press

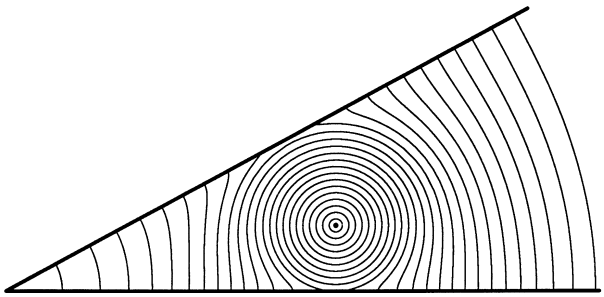

FIGURE 2. Injection is at $z = 5 + i$ into a corner formed by the half-lines $\arg z = 0$ and $\arg z = 1/2$. There is an air vent at the vertex, so there is the same pressure on both free boundaries when two are present. With an area πr^2 injected, outlines of the blob of fluid are drawn at increments of 0.1 in r up to $r = 2.5$. All the air is expelled when $r = 2.37129$. See text for further details.

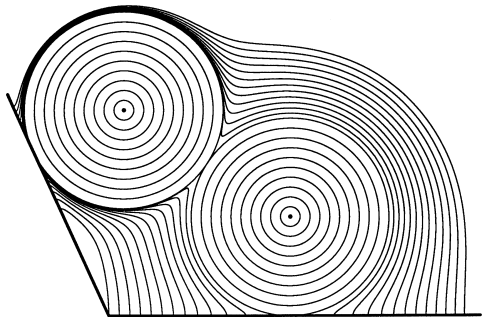

FIGURE 3. Injection is at $z = a_1 = e^{i/2}$ and $z = a_2 = e^{3i/2}$ into a corner formed by the half-lines $\arg z = 0$ and $\arg z = 2$, and there is an air vent at the vertex. With an area πr_j^2 injected at $z = a_j$, we have equal injection rates at both points until $r_1 = r_2 = \sin(1/2) = 0.479426$ when the expanding circular blobs touch both each other and the sides. All further injection is at $z = a_1$, and the point where the inner free boundary meets $\arg z = 0$ reaches the vertex when $r_1 = 0.758392$. Outlines of the blob are drawn for 10 equal increments in r_1 and r_2 up to $r_1 = r_2 = \sin(1/2)$, followed by a further 12 equal increments in r_1 up to $r_1 = 0.758392$.

process and (2.24) for $1 < \alpha < 2$, we find a local expansion for $f(\zeta)$ of the form $f(\zeta) = \zeta^{\alpha-1}(a + b\zeta + c\zeta^2 + \cdots)$, but a closer examination reveals that $a = 0$. For $0 < \alpha < 1$ we obtain $f(\zeta) = \zeta^{\alpha}(a + b\zeta + c\zeta^2 + \cdots)$, but now $a \neq 0$.

3 Examples

Figure 2 shows a simple example of injection into a corner, with an air vent at the vertex so that we have equal pressures on both free boundaries when two are present. The angle is $\alpha\pi = 1/2$, and the injection is at the single point $z = 5 + i$. With an area πr^2 injected, we have an expanding circular blob as r increases to 1, when it comes into contact with $\arg z = 0$. Further increase in r results in the blob coming into contact with $\arg z = 1/2$ when $r = 1.47156$ (at the point $z = 4.25888 + 2.32664i$), and the air in the corner is all expelled when $r = 2.37129$.

In Figure 3, we have an obtuse corner with $\alpha = 2/\pi$, so the angle is 2 radians. There are two injection points at $z = a_1 = e^{i/2}$ and $z = a_2 = e^{3i/2}$, and there is an initial phase

https://doi.org/10.1017/S0956792501004570 Published online by Cambridge University Press

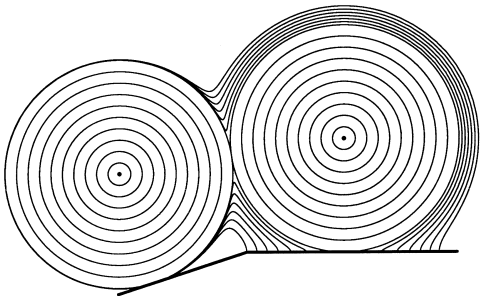

FIGURE 4. With $\alpha = 1.1$, injection is at $z = a_1 = e^{\alpha\pi i/4}$ and $z = a_2 = e^{3\alpha\pi i/4}$, the half-lines are $\arg z = 0$ and $\arg z = \alpha\pi$, and there is an air vent at the vertex. With an area πr_j^2 injected at $z = a_j$, we have equal injection rates at both points until $r_1 = r_2 = \sin(\alpha\pi/4) = 0.760406$ when the expanding circular blobs touch both each other and the sides. All further injection is at $z = a_1$, and the point where the inner free boundary meets $\arg z = 0$ reaches the vertex when $r_1 = 0.879511$. Outlines of the blob are drawn for 10 equal increments in r_1 and r_2 up to $r_1 = r_2 = \sin(\alpha\pi/4)$, followed by a further 6 equal increments in r_1 up to $r_1 = 0.879511$.

with equal injection rates at both points so we then have two expanding circular blobs. With an area πr_j^2 injected at $z = a_j$, these growing blobs touch both each other and the sides when $r_1 = r_2 = \sin(1/2) = 0.479426$. We then cease injecting at $z = a_2$ but continue at $z = a_1$, supposing there to be an air vent at the vertex so that the pressures on the two free boundaries now present are equal. As expected, the growing blob spreads faster along $\arg z = 0$ than it does along $\arg z = 2$, and we find that the lower end of the inner free boundary reaches the vertex when $r_1 = 0.758392$. Any further increase in r_1 will result in this point moving up the half-line $\arg z = 2$, a motion that the present analysis cannot follow, for images now lead to a configuration with a fluid region of infinite connectivity on a Riemann surface. If we really do have an air vent just at the corner, the trapped air cannot now escape (a situation to be avoided in the injection moulding context) and the equal-pressures assumption will no longer be tenable, but solving for the further motion with this assumption still in place will tell us where an air vent should be placed on $\arg z = 2$ in order to ensure that all the air *is* expelled.

The scenario shown in Figure 4 is similar to that in Figure 3, but we now have a reflex angle with $\alpha = 1.1$. The injection points are at $z = a_1 = e^{\alpha\pi i/4}$ and $z = a_2 = e^{3\alpha\pi i/4}$, and injecting at equal rates yields two growing circular discs that come into contact with both each other and the solid boundaries when $r_1 = r_2 = \sin(\alpha\pi/4) = 0.760406$. Continuing to inject only at $z = a_1$ and supposing there to be an air vent at the vertex, the end of the free boundary moving along $\arg z = 0$ towards the vertex now reaches it when $r_1 = 0.879511$.

The special case $\alpha = 1$ for which elliptic functions are required just involves a straight boundary and, invoking images, is merely a particular instance of flow with a doubly-connected fluid region and no solid boundaries present where there happens to be symmetry about a line. (One may consider the case $\alpha = 1$ of the scenario in Figures 3 and 4 with no difficulty; the air escapes if the vent is correctly placed.) The special case $\alpha = 2$ that also requires elliptic functions is of a different character, and we give an example with such an α which, like that in Figure 6 of Richardson (2001b), has a cusp

https://doi.org/10.1017/S0956792501004570 Published online by Cambridge University Press

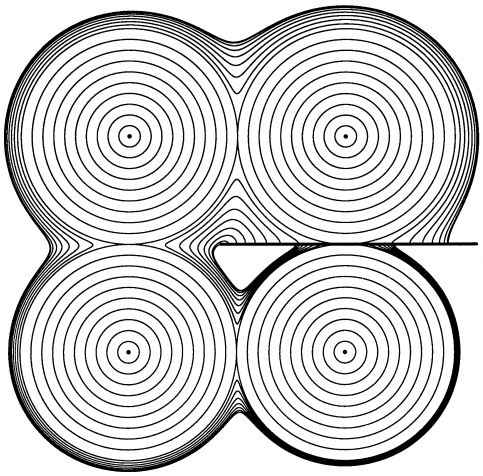

FIGURE 5. The boundary is the portion $x > -0.151121$ of the x-axis, and there is injection at the points $a_1 = +1-i, a_2 = -1-i, a_3 = -1+i$ and $a_4 = +1+i$. With an area πr_j^2 injected at $z = a_j$, we have equal injection rates at all four points until $r_1 = r_2 = r_3 = r_4 = 1$, and then the rates of increase of r_1, r_2, r_3 and r_4 are in the ratios $1:2:3:4$ until $r_4 = 1.18628$, with the pressures on the two free boundaries equal. Outlines are drawn for increments of 0.1 in each of the r_j as they increase from 0 to 1 for the first stage of the motion. For the second stage, set $r_4 = 1 + 0.18628p(2-p)$. Outlines are then drawn for increments of $1/8$ in p from $p = 1/8$ to $p = 1$. See text for further details.

appearing at a solid boundary as a result of injection. It will also serve to illustrate some mathematical subtleties.

We will eventually be modifying the geometry a little, but begin with a situation that is represented by our basic assumptions when $\alpha = 2$, so we have a solid boundary just along the positive x-axis. Consider injection at the four points $z = \pm 1 \pm i$; we number these clockwise starting in the fourth quadrant, so $a_1 = +1-i, a_2 = -1-i, a_3 = -1+i, a_4 = +1+i$, and have πr_j^2 as the area injected at $z = a_j$. Injecting at equal rates at all four points initially, we reach a configuration of four touching circular discs when $r_1 = r_2 = r_3 = r_4 = 1$. Now continue injection with the rates of increase of r_1, r_2, r_3 and r_4 in the ratios $1:2:3:4$; we are, of course, supposing that the pressures on the two free boundaries that are now present are kept equal. The fluid region grows as a single entity that spreads along the upper side of the boundary $\arg z = 0$ faster than it does along the lower side, and we find that the point where the inner free boundary meets the upper side reaches the vertex at $z = 0$ when $r_4 = 1.17423$. Further injection with the present geometry would have this point moving round to the lower side of the boundary (producing a situation that the present methods cannot analyse), but what if the boundary extended a little to the left of $z = 0$, so it occupied the portion $x > -a$ of the x-axis for some $a > 0$? Then this point continues to move to the left on the upper side of the x-axis. Pursuing this possibility for increasing a, we find that if the injection continues as before and the solid boundary is the portion $x > -0.151121$ of the x-axis, then the free boundary changes from being perpendicular to the solid boundary to being tangential to it as it reaches the vertex at $x = -0.151121$, and this occurs when $r_4 = 1.18628$. This evolution is shown in Figure 5. The free boundary moves very rapidly when near the vertex and a

https://doi.org/10.1017/S0956792501004570 Published online by Cambridge University Press

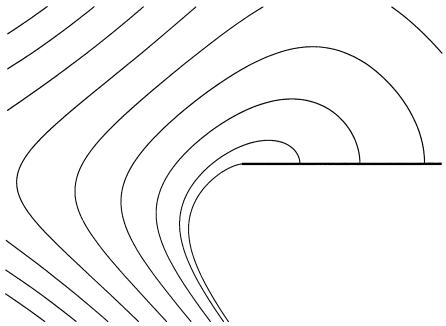

FIGURE 6. The region $-0.45 < x < 0.1, -0.2 < y < 0.2$ in Figure 5.

nonlinear scaling has been used for the increments in r_4 for this figure (see the caption) so that a reasonable number of curves are drawn near the most interesting state. On the scale of Figure 5, this detail is not visible, but a close-up of the region near the vertex appears in Figure 6.

The computations required for this example are rather delicate because, once the free boundary has moved to the left of the origin, equation (2.21) is no longer correct. If one visualizes the z-plane in Figure 1 for $\alpha = 2$, one sees that the origin is then a point on the boundary of the fluid region D, the harmonic function $\log|z|$ used to derive (2.21) has a singularity on this boundary, and there is an extra term in this equation. Moreover, this term involves the unknown value of the harmonic function ϕ at the origin, so the correct equation is not very helpful! One way round the difficulty is to use the function $\log|z+a|$ for some $a > 0$ instead of $\log|z|$ in this derivation (so we are effectively moving the vertex to $z = -a$) and choose a carefully so that $z = -a$ is neither within D nor on its boundary. A simpler solution is to exploit the translation invariance in this problem and, instead of moving the vertex to the *left* a distance a, we move the injection points to the *right* a distance a, now choosing a carefully so that the origin is neither within D nor on its boundary, and (2.21) is therefore correct. As we increase r_4 (with the other r_j known in terms of r_4) we must adjust a so that this condition continues to hold. When near the limiting situation, we can then add in two equations to those being solved (one specifying that the free boundary passes through the origin, and the other that it has a tangent parallel to the x-axis there) and thus solve for the extra parameters a and r_4 needed for the final state in Figures 5 and 6. Once this process has determined that we then need $a = 0.151121$, this value can be used for all subsequent computations with this configuration.

Similar concerns arise with the examples of Figures 3 and 4, for the vertex at the origin there is not inherent in the mathematics; this merely ensures that the fluid is in contact with a solid along two line segments in specified directions. With further injection at $z = a_1$, it is possible to continue these solutions and have one end of the inner free boundary moving to the left of the origin along the x-axis, while the other continues to move along $\arg z = \alpha\pi$ towards the origin. With the pressures on the two free boundaries still supposed to be equal, one anticipates that one can again produce a situation with a cusp appearing at a solid boundary, on $\arg z = \alpha\pi$ in Figure 3 but on the x-axis in Figure 4. However, to analyse this motion, we no longer have a translation invariance to

https://doi.org/10.1017/S0956792501004570 Published online by Cambridge University Press

help, and (2.21) must be modified. This modified form is still obtained by using for $l(x, y)$ in (2.20) a time-independent function with $\partial l/\partial n = 0$ on $\Gamma_0 \cup \Gamma_\alpha$ that is harmonic in the closure of D, but a simple choice of the form $\log|z|$, or $\log|z + a|$, is no longer admissible.

4 Concluding remarks

In Richardson (2001b), an effective solution procedure was presented for Hele-Shaw flows with time-dependent free boundaries in a corner or around a wedge when the fluid (liquid) is present at the vertex, and a constant-pressure condition is relevant at the free boundary. In the present paper, a similar situation, but with air trapped near the vertex, has been analysed. An essential assumption in both circumstances is that the liquid be in contact with both half-lines forming the solid boundary only along a single segment, so no air is trapped away from the vertex. However, examples show that some motions which satisfy this assumption inevitably evolve to a state where it is no longer valid and we have air trapped along one or both sides of the corner or wedge. If the angle $\alpha\pi$ is such that $\alpha = 1/n$ for some positive integer n, we can invoke images and consider an equivalent problem in the z-plane with no solid boundaries present, but with a fluid region that is multiply-connected. Such problems can be solved by the methods of Richardson (2001a) – indeed, some of the examples given in this reference can be reinterpreted as flows in corners. If α is not of this special form, images lead us to consider flows on Riemann surfaces with the fluid occupying a multiply-connected region, and the analysis of this situation requires methods that are an amalgam of those already developed.

Acknowledgement

The numerical computations required for this paper were performed using *Mathematica* (Version 3), and its graphics facilities were employed for the production of the figures.

References

[1] Bowman, F. (1961) *Introduction to Elliptic Functions with Applications*. Dover.
[2] Hermite, C. (1912) *Œuvres de Charles Hermite*, Tome III. Gauthier-Villars.
[3] Rainville, E. D. (1971) *Special Functions* (2nd edition). Chelsea.
[4] Richardson, S. (1994) Hele-Shaw flows with time-dependent free boundaries in which the fluid occupies a multiply-connected region. *Euro. J. Appl. Math*. **5**, 97–122.
[5] Richardson, S. (1996) Hele-Shaw flows with free boundaries driven along infinite strips by a pressure difference. *Euro. J. Appl. Math*. **7**, 345–366.
[6] Richardson, S. (2000) Plane Stokes flows with time-dependent free boundaries in which the fluid occupies a doubly-connected region. *Euro. J. Appl. Math*. **11**, 249–269.
[7] Richardson, S. (2001a) Hele-Shaw flows with time-dependent free boundaries involving a multiply-connected fluid region. *Euro. J. Appl. Math*. **12**, 571–600.
[8] Richardson, S. (2001b) Hele-Shaw flows with free boundaries in a corner or around a wedge. Part I: Liquid at the vertex. *Euro. J. Appl. Math*. **12**, 665–676.